Structural Engineering and Mechanics, *Vol. 50, No. 3 (2014) 287-304*
DOI: http://dx.doi.org/10.12989/sem.2014.50.3.287

Wave load resistance of high strength concrete slender column subjected to eccentric compression

M. Jayakumar*[1] and B.V. Rangan[2a]

[1]Department of Civil and Construction Engineering, Curtin University, Sarawak. Malaysia
[2]Faculty of Engineering and Computing, Curtin University, Perth, Australia

(Received November 27, 2012, Revised December 31, 2013, Accepted March 5, 2014)

Abstract. A computer based iterative numerical procedure has been developed to analyse reinforced high strength concrete columns subjected to horizontal wave loads and eccentric vertical load by taking the material, geometrical and wave load non-linearity into account. The behaviour of the column has been assumed, to be represented by Moment-Thrust-Curvature relationship of the column cross-section. The formulated computer program predicts horizontal load versus deflection behaviour of a column up to failure. The developed numerical model has been applied to analyse several column specimens of various slenderness, structural properties and axial load ratios, tested by other researchers. The predicted values are having a better agreement with experimental results. A simplified user friendly hydrodynamic load model has been developed based on Morison equation supplemented with a wave slap term to predict the high frequency non-linear impulsive hydrodynamic loads arising from steep waves, known as ringing loads. A computer program has been formulated based on the model to obtain the wave loads and non-dimensional wave load coefficients for all discretised nodes, along the length of column from instantaneous free water surface to bottom of the column at mud level. The columns of same size and material properties but having different slenderness ratio are analysed by the developed numerical procedure for the simulated wave loads under various vertical thrust. This paper discusses the results obtained in detail and effect of slenderness in resisting wave loads under various vertical thrust.

Keywords: concrete column; wave loads; eccentric compression; Moment-Thrust-curvature; secondary moments

1. Introduction

Model tests and field experience of offshore structures have shown that loads on large surface piercing structures, such as columns of concrete gravity structures, in steep wave condition are considerably larger than those assumed in conventional design calculations. In extreme, near-breaking wave conditions, offshore platforms exhibit significant resonant response called ringing. The ringing effect occurs like irregularly spaced bursts of response at the natural frequency of the structure. The bursts are superimposed on the response that can be predicted by traditional linear theory. The impact force that causes the response is associated with the vertical or near-vertical

*Corresponding author, Senior Lecturer, E-mail: m.jayakumar@curtin.edu.my
[a]Emeritus Professor

http://www.techno-press.org/?journal=sem&subpage=8 ISSN: 1225-4568 (Print), 1598-6217 (Online)

free surface of the wave front as the wave steepens. This impulsive load resulting from the crest of breaking or near breaking waves interacting with the structure is significant in magnitude, and must be considered in design. The “user-friendly” simplified hydrodynamic load model, which can predict impact loads and enable practical applicability without involving tedious computational efforts developed by the author, has been used to predict non-dimensional wave load coefficients at various water depths.

In the literature several analytical procedures as well as experimental results are available for pin ended column in single curvature, double curvature and biaxial bending under axial or eccentric compression whereas only a few details are available for high strength concrete cantilever columns subjected to varying horizontal loading such as wave loading, along the length of the column together with eccentric compression. Berera (2013) conducted the experimental studies to investigate the second order effect on slender HSC column subjected to constant axial load and monotonic lateral forces and concluded, the second order effects have major influence on the deformation capacity of the columns. Leite (2013) analysed the ultimate strength and deformed shape of the column under compression and uniaxial bending and compared results obtained by their calibrated numerical model with the results by the simplified methods proposed in EC-2 (2004) and ACI-318 (2008). Doren (2009) developed the comprehensive nonlinear finite element model to predict the stress-strain behaviour and load resistance for conventional R.C columns subjected to concentric loading and verified with the available test results published by seven different researches. Hugo Rodrigues (2012) compared the performance of different nonlinear modelling strategies to simulate the response of R.C columns subjected to axial load combined with cyclic biaxial horizontal loadings. Significant differences were found in the strength degradation and energy dissipation with three modelling strategies used. Bouchaboub (2013) applied the finite difference method to calculate the load corresponding to a specific deflection for the columns with hinged extremities by connecting both material and geometric nonlinearities. Sarker and Rangan (2000) developed the numerical procedure based on Moment-thrust-curvature approach to study the behaviour of the columns in double curvature mode due to unequal eccentricity at the both ends. This paper briefly describes the numerical method to predict the strength and deflection of high strength concrete cantilever column subjected to eccentric compression and lateral loads of varying magnitude along the length of the column. The deformation is assumed to be small such that curvature can define by second derivation of deflection and the column section has adequate transverse reinforcements for confinement as recommended by ACI 318-08 (2008). The described numerical method is user friendly and ease application for any given support conditions and lateral load profile.

2. Simplified wave impact load model

A simplified wave impact load model by Jayakumar (2010) to predict the additional impact (Ringing) load due to a high frequency steep wave at near breaking condition is briefly described here. The wave load model is developed based on Morison’s equation supplemented with a wave slap term. Stokes fifth order wave theory is used to predict the water particle kinematics. The simplified wave impact load model is validated with experimental results by Zou and Kim (1995). The validation of load model shows good agreement with the experimental and analytical values obtained by Zou and Kim (1995). A computer program has been formulated based on the model to obtain the wave loads at all discretised nodes, along the length of column from instantaneous free water surface to the bottom of the column at mud level for the given depth of water, wave height, period of time and size of the column and to calculate the non-dimensional load coefficient for all nodes. In case of large, steep waves the basic Morison equation formulation has been found to be unable to accurately predict the total wave load acting on a cylindrical member. The response of the structure will be amplified due to resonant effects when the frequency of the wave loading is close to the natural period of the structure. As proposed by Davies *et al*. (1994) and followed by Baudic *et al*. (2000), an additional term has been added to the Morison's force expression to predict the "Slam" force or impact force.

The total horizontal force due to wave loading is

$$F(t) = F_m(t) + F_s(t) \tag{1}$$

where $F(t)$ is the time dependent load vector given by the sum of Morison force $F_m(t)$ with modified Morison equation by Sarapkaya and Isaacson (1981) and Slam force $F_s(t)$. The method proposed here incorporates Stokes fifth order theory to estimate the water particle kinematics under steep regular wave. Slam force is also obtained by using the same kinematics

2.1 Morison equation force

The Morison equation was developed by Morison *et al.* (1950) in describing the horizontal wave forces acting on a vertical pile that extends from the bottom through to the free surface. Morison *et al*. (1950) proposed that the force exerted by unbroken surface waves on a vertical cylindrical pile that extends from the bottom through to the free surface is composed of two components, inertia and drag. Combining the inertia and drag components of force, the Morison equation force F_m is written as

$$F_m = C_m \rho \frac{\pi}{4} D^2 \frac{du}{dt}.ds + C_d.\frac{1}{2}\rho D\left|u\right|u.ds \tag{2}$$

where,

C_m = inertia coefficient
C_d = drag coefficient
ρ = density of water
D = diameter of the cylinder
u = water particle velocity
ds = segmental length of the cylinder

2.2 Slap or slam force

Assume the steep, near breaking wave as shown in Fig. 1 for analyzing the slap or slam load on a vertical cylinder of diameter, D. A small elemental strip of length dy at the height of η from the still water level (SWL) is considered and u is the water particle velocity on the wave front at the point of impact on the strip, which may be approximated and calculated by the Stokes fifth order wave theory. The immersion diametrical distance for the strip of length dy at η from the still water level is S which is defined in Fig. 1 and η_c is the height of wave crest from SWL. The additional load due to the steep wave at near breaking, is fairly predicted by a simplified term

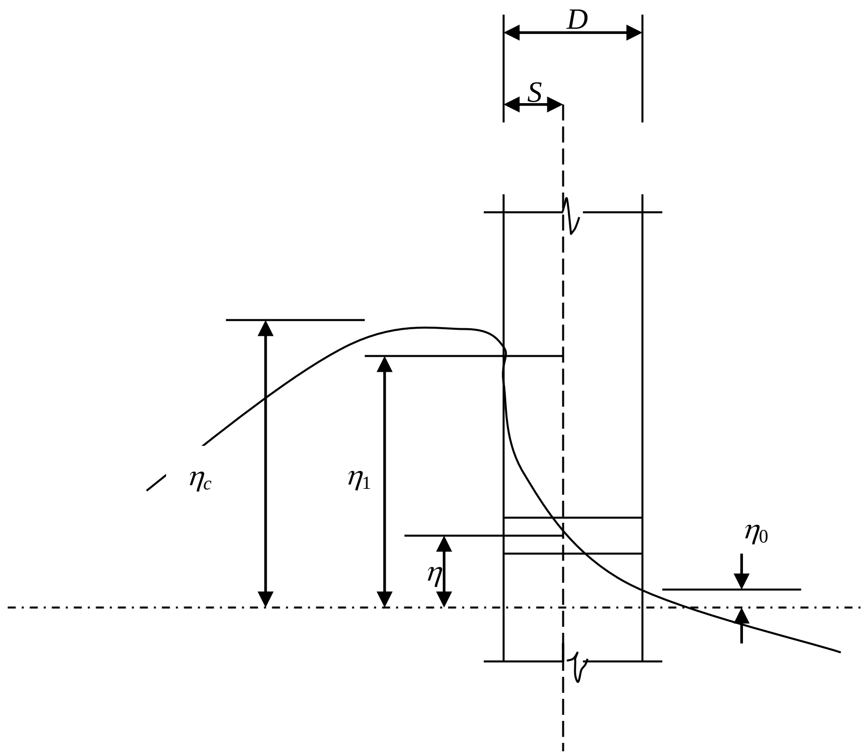

Fig. 1 Wave impact on a vertical cylinder

$$F_s = 1/2\,\rho D \int_{d+\eta_0}^{d+\eta_1} u^2 C_s(y)\,dy \tag{3}$$

where u is the water particle velocity on the wave front at point of impact, η_0 and η_1 are the lower and upper contact points of the wave free surface on the cylinder, as shown in Fig. 1, C_s is the slam or slap coefficient and d is the depth of water from SWL to mud level. D is the diameter of the cylinder and ρ is the density of water. The slap coefficient C_s is proportional to the rate of change of added mass with immersion diametrical distances. Campbell and Weynberg (1979) experimentally derived slap or impact coefficient C_s is given by,

$$C_s = 5.15\left[\frac{D}{D+19S} + \frac{0.107S}{D}\right] \tag{4}$$

where S is the immersion diametrical distance defined in Fig. 1. A typical mean value of C_s may be taken as 3.5 even though considerable scatter in the coefficient has been found in the experimental values.

2.3 Wave Kinematics model

In this study, Stokes fifth-order wave theory is used to obtain the water particle kinematics of steep wave. The wave profile is assumed as a near breaking, regular wave in deep sea condition. Once the potential function Φ is known, the water-particle kinematics is obtained by spatial differentiation. The fifth-order velocity potential is written in a series form as

$$\Phi = \frac{c}{k}\sum_{n=1}^{5}\lambda_n \cosh nks \sin n\Theta \tag{5}$$

where c is celerity, k wave number, s is the depth of the section measured from seabed level. $\Theta=(kx-\omega t)$ is the phase angle and λ is a non-dimensional coefficient the non-dimensional coefficients.

2.4 Illustrative column analysis by the proposed Wave Load Model

The column of diameter 3.34 m subjected to the wave of height 15.25 m was analyzed by the proposed simplified wave impact load model. The depth of water from still water level is 30.5 m and wave period is 10 seconds. As recommended by designers and the British Standard institute, the selected inertia coefficients C_m, drag Coefficient C_d and slap coefficients C_s are 1.7, 0.7 and 3.5 respectively. The calculated results by Jayakumar (2004) are shown in Table 1. The non-dimensional wave load profile was plotted and shown in Fig. 2.

The lateral wave loads were applied and incremented in accordence to the nondimentional wave load coefficients shown in Table 1, in the illustrative example dicussed in the later section "Column Analysis".

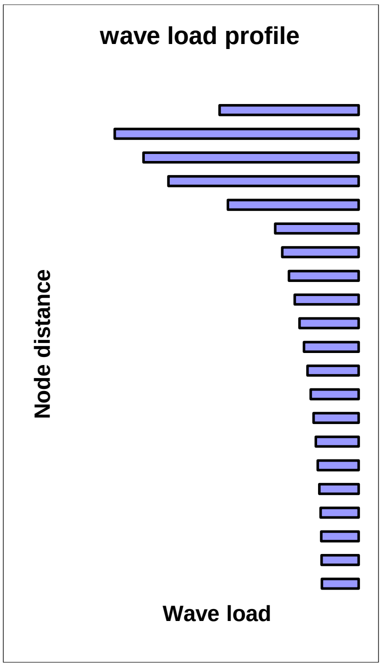

Fig. 2 Total wave load profile on the column height

Table 1 Wave loads and load coefficients for the nodes

Depth m	Morison unit force *N*	$F_{m,}$ Morison force *N*	Velocity at T_m m/sec	$F_{s,}$ Slap force *N*	*F*, Total force *N*	Wave load coeff.
38.125	84512.86	80540.76	3.79	80012.13	160552.9	0.56976
36.219	75833	144537.7	3.51	137252.9	281790.6	1
34.313	68248.78	130082.2	3.26	118397.5	248479.7	0.881788
32.406	61606.59	117422.2	3.03	102280.5	219702.6	0.779666
30.5	55788.58	106333	2.83	44611.86	150944.9	0.535663
28.594	50686.62	96608.7	2.65	0.0	96608.7	0.342839
26.688	46212.69	88081.39	2.48	0.0	88081.39	0.312577
24.781	42290.27	80605.25	2.34	0.0	80605.25	0.286047
22.875	38859.97	74067.1	2.21	0.0	74067.1	0.262844
20.969	35865.49	68359.62	2.09	0.0	68359.62	0.24259
19.062	33259.33	63392.28	1.99	0.0	63392.28	0.224962
17.156	31004.8	59095.15	1.89	0.0	59095.15	0.209713
15.25	29066.88	55401.47	1.81	0.0	55401.47	0.196605
13.344	27417.2	52257.18	1.74	0.0	52257.18	0.185447
11.438	26031.87	49616.74	1.68	0.0	49616.74	0.176077
9.531	24890	47440.34	1.63	0.0	47440.34	0.168353
7.625	23978.29	45702.62	1.59	0.0	45702.62	0.162186
5.719	23281.57	44374.67	1.56	0.0	44374.67	0.157474
3.813	22790.69	43439.06	1.54	0.0	43439.06	0.154154
1.906	22498.71	42882.54	1.53	0.0	42882.54	0.152179
0	22401.9	21349.01	1.52	0.0	21349.01	0.151524

3. Numerical model to assess the lateral strength of column

This section describes a non-linear numerical method to predict the strength and deflection of high strength concrete rectangular columns subjected to wave impact loads and vertical thrust. A computer program was developed to implement the method. The developed method predicts the response of high strength concrete columns under prescribed eccentric compression, up to failure for simulated lateral loads.

3.1 Moment-Trust-Curvature (M_i – N - k) relationship

Moment-Thrust-Curvature, relationship for specified values of axial thrust are prerequisites to the method of analysis described. For this purpose, the column cross-section is first divided into a number of strips of equal heights as shown in Fig. 3. For the nominated value of an axial load *N*, a value of the strain at the extreme compressive fiber of concrete ε_{cc}, is then prescribed. For this value of ε_{cc} a trial value of neutral axis depth, d_n is guessed and the strains in each concrete strips and reinforcing steel layers are obtained from the assumed stress-strain relationship for concrete and steel, respectively. The stress at the centroid of the strip is assumed to be constant throughout its depth and is multiplied by its area to obtain the force in that strip. Similarly, the force in the

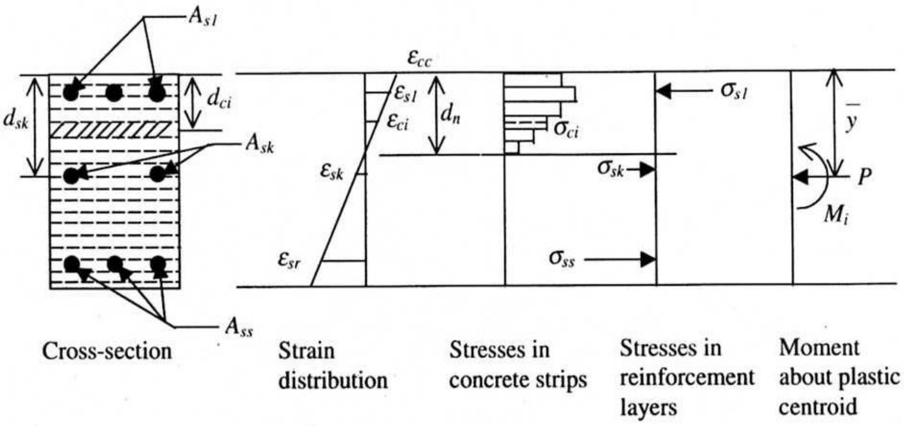

Fig. 3 Analysis of column cross-section

reinforcement at any level of is obtained as the product of the stress at that level and the respective area of steel. The forces in all the concrete strips and steel layers shown in Fig. 3 are summed algebraically to obtain the net axial force *P* acting on the section as in Eq. (6).

$$P = \sum_{i=1}^{m} \sigma_{ci} \mathrm{A}_{ci} + \sum_{k-1}^{s} \sigma_{sk} \mathrm{A}_{sk} \tag{6}$$

where,

σ_{ci} = stress in the *i*-th strip of concrete
A_{ci} = area of the *i*-th strip of concrete
m = total number of concrete strips
σ_{sk} = stress in the *k*-th layer of reinforcement
A_{sk} = area of steel in the *k*-th layer of reinforcement
s = total number of reinforcement layers

The net axial force *P* is now compared with the nominated value *N*. If the difference between these values is not within a prescribed tolerance, a new position of the neutral axis is guessed and the process is repeated. When the correct position of the neutral axis is obtained, the internal moment M_i about the plastic centroid for that value of *N* is calculated. The moment of the force in any concrete strip or in reinforcement layer is the product of the force and the distance between the centroid of that strip or layer and the plastic centroid of the cross-section. The total moment of the section is then obtained by summing the moments of the individual concrete strips and reinforcements. The corresponding curvature is calculated as the slope of the strain profile across the cross section shown in Fig. 3.

$$M_i = \sum_{i=1}^{m} \sigma_{ci} \mathrm{A}_{ci} (\bar{y} - d_{ci}) + \sum_{k-1}^{s} \sigma_{sk} \mathrm{A}_{sk} (\bar{y} - d_{sk}) \tag{7}$$

where,

d_{ci} = depth of *i*-th concrete strip from the compressive face
d_{sk}= depth of the *k*-th layer of reinforcement from the compressive face
$\bar{y}$= depth of the plastic centroid from the compressive face

$$k = \frac{\varepsilon_{cc}}{d_n} \tag{8}$$

The entire process is repeated for different values of extreme compressive fiber strain, ε_{cc} increasing by a prescribed incremental value and a complete set of M_i and k values are calculated for the specified value of N until the maximum value of M_i is reached. As the column behavior is defined by the M_i - N - k relationship of the cross section, the accuracy of the method of analysis also depends on how accurately this relationship is developed.

3.2 Stress- Strain relationship

In order to use the described procedure to predict the strength and response of columns, it is important that the appropriate stress-strain relationships for concrete and reinforcing steel are used to develop the moment-curvature relationships of the cross section. The stress-strain relationship used in this analysis was proposed by Popovics (1973) and subsequently modified by Collins (1992) to ensure a steeper descending part for high strength of concrete.The modified relationship is expressed in terms of f'_c by the following equations. However, the strength of concrete in a column differs from that in a cylinder due to differences in size, vibration during casting, curing, loading rate etc. To take into account these differences, a factor K_3 is applied to the cylinder stress to obtain the concrete stress in a column. Many researchers showed that K_3 can be suitably expressed in terms of f'_c. The proposed sets of equations by Attard and Stewart (1997) as below are used in this study.

$$K_3 = 1.05 - 0.0009 f_{cm} \tag{9}$$

$$f_{cm} = f_c' + 7.5 \text{ MPa} \tag{10}$$

The stress-strain relationship of the reinforcing steel is assumed as elastic-perfectly plastic both in tension and compression.

3.3 Deflection of HSC column

The column length is discretised into a number of rigid segments of finite length to predict the deflected shape under the nominated vertical load and lateral horizontal loads. Deflection of the plastic centroid of the cross section at the nodes connecting the rigid segments are first calculated by an iterative procedure and then they are connected together to obtain the column deflected shape under any particular load. Let us consider a column of effective length L subjected to an axial load N with end eccentricity e at the top as shown in Fig. 4. The column is first discretised into (n-1) number of rigid segments of length ΔL where, n is the number of nodes. The curvature of the deflected shape at any point is defined as the rate of change of slope θ at that point. If the length of the segments is sufficiently small, then the slope θ_j and curvature k_j at any node j can be represented in terms of the node deflections by the following equations

$$\Delta\theta_j = \frac{(v_{j+i} - v_j) - (v_j - v_{j-i})}{\Delta L} \tag{11}$$

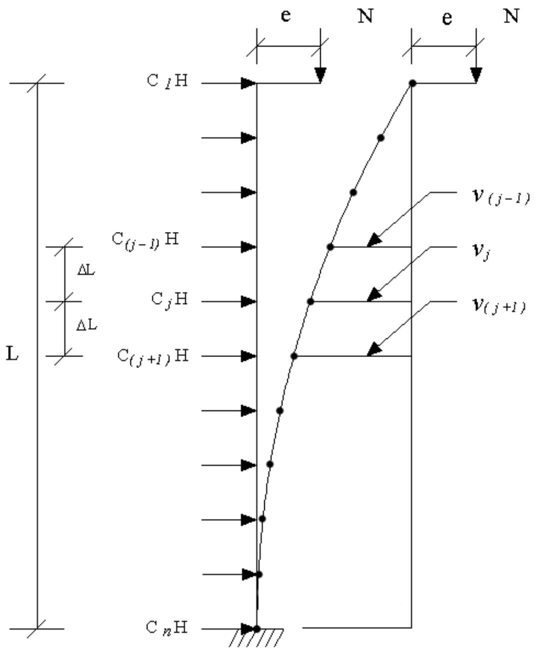

Fig. 4 Deflected shape of the column

$$k = \frac{\Delta\theta_j}{\Delta L} = \frac{v_{j+1} - 2v_j + v_{j-1}}{(\Delta L)^2} \tag{12}$$

Eq. (11) can be arranged as

$$v_{j+1} = k_j (\Delta L)^2 + 2\, v_j - v_{j-1} \tag{13}$$

Eq. (13) can be rewritten in generalized form as

$$v_j = k_{j-1}(\Delta L)^2 + 2v_{j-1} - v_{j-2} \tag{14}$$

where,

$\Delta\theta_j$ = change of slope at any node j in length ΔL

k_j = curvature at any node j

v_j = deflection of node 1 from the new location of node j

The numerical computation starts from node 1, where deflection (v_1) of node 1 from the new location of node 1 is zero. A control slope θ_1, which is the slope of the first segment, is then assumed and the deflection at node 2 is calculated, which is equal to the product of θ_1 and the length of the segment ΔL. Now the deflections at all the subsequent nodes are calculated according to Eq. (14). The value of curvature k_{j-1} is obtained from appropriate *M-k* relationship. The external moment at any node j is then calculated with reference to Fig. 4.

$$M_{ej} = N\,(e + v_j) + [C_1H\,(j-1) + C_2H\,(j-2) + \ldots\ldots + C_jH\,(j-j)]\ \Delta L \tag{15}$$

where,

Table 2 Calculated values with experimental results by Azizinamini (1994)

Column No.	Calculated Results			Experimental Data			N/Po	Test/Calculated	
	M(kNm)	H_u(kN)	Defl(mm)	M(kNm)	H_u(kN)	Defl(mm)		M	H_u
TC 3.1	216	196.42	6.57	248.6	228.06	5.08	0.2	1.15	1.16
TC 3.2	208	188.76	6.55	238.29	217.89	5.84	0.2	1.15	1.15
TC 3.3	294	264.09	7.64	272.05	245.16	6.64	0.2	0.93	0.93
TC 3.4	290	260.65	7.72	295.84	268.26	6.1	0.2	1.02	1.03
TC 3.5	293	262	7.71	267.52	241.24	6.35	0.2	0.91	0.92
TC 3.6	293	263.45	7.73	288.81	260.05	7.11	0.2	0.99	0.99

M_{ej} = external moment at any node j
$C_1, C_2 \ldots C_j$ = wave load coefficients
H = Assumed incremented wave load for nodes

The main objective of this numerical procedure is accounting the secondary moment due to the vertical load in the deflected mode resulting from the p-Δ effect. This is duly accounted in the Eq. (15), for the external moment at any node j as $N(e + v_j)$. In the term $N(e + v_j)$ in Eq. (15), $N.e$ represents the primary moment due to the applied vertical load N resulting from the given eccentricity e and the term $N.\ v_j$ represents the secondary moment due to p-Δ effect.

The developed numerical model has been validated by Jayakumar (2004), with the available experimental results of 36 reinforced rectangular columns and 4 circular columns of various slenderness, structural properties and compressive thrust levels, tested by other researchers. The predicted values are having a better agreement with available experimental results. As an example, the validated results of calculated values for 6 column specimens with the experimental results reported by Azizinamini (1994) are shown in Table 2.

4. Analytical simulations

In order to conduct a study using the numerical method developed by the authors, reinforced concrete column sections with various grade of concrete and contained different percentage of longitudinal reinforcement were selected and assumed to be contained adequate transverse reinforcement to ensure the failure only in flexure. The columns were assumed to be fixed at bottom and free at the top. From the results of this study, some conclusions and suggestions are made to design reinforced concrete slender columns primarily to resist the lateral loads along with eccentric compression. The variables used for this study are concrete strength, slenderness ratio, vertical load ratio and longitudinal reinforcement ratio. The two different column cross-sections with different reinforcement ratios were used.

The parameters varied in the range as mentioned below in this study.

N / P_0 = 0.1 to 0.6
L_e / r = 40, 60, 80 and 100.
f_c' = 40, 60, 80 and 100 MPa.
p = 1.0%, 2.5% and 4.0%.

where,

N / P_0 = Vertical load ratio in which N and P_0 are applied vertical load squash load of the

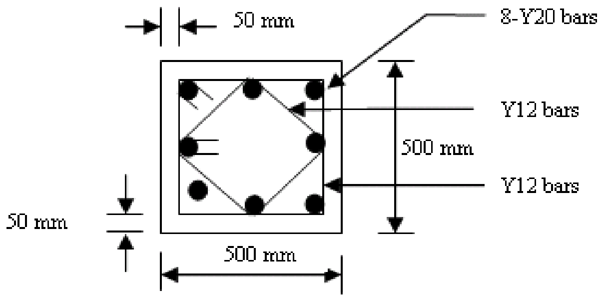

Fig. 5 Column cross-section 500 mm×500 mm

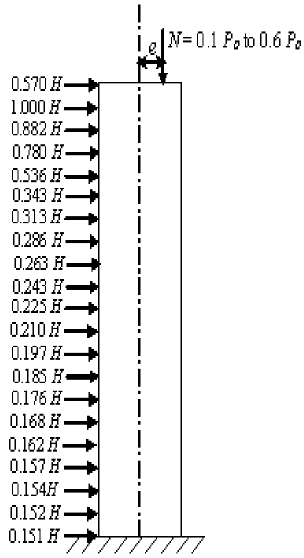

Fig. 6 Column shows lateral and vertical loads

column section.

L_e / r = Slenderness ratio in which L_e and r are the effective length and radius of gyration respectively; r is taken as 0.3D for a rectangular sections.

f_c' = Concrete compressive strength and

p = Longitudinal reinforcement ratio = A_s/bD in which A_s is the total area of longitudinal reinforcement.

Since the columns are assumed to be fixed at bottom and free at top, the effective length was considered as twice the actual length in slenderness calculations. The column cross-section 500×500 mm with reinforcement details is shown in Fig. 5.

The entire length of the column was discretised into 20 equal segments and nodes were subjected to the lateral wave loads varied hyperbolically from top to bottom nodes. The lateral wave loads were applied in terms of calculated wave load coefficients shown in Table 1. The lateral and vertical loads considered in this study are shown in Fig. 6. The lateral loads assumed in terms of wave load coefficients were incremented up to failure under each vertical load as the percentage of squash load P_0 of the column sections considered.

For obtaining the best results, the lateral load H shown in Fig. 6 incremented as small as 0.000025 H_0. Whereas H_0 is the hypothetical maximum lateral load expected to resist by the column of given material and structural properties without considered the secondary moments resulting by the vertical load due to deflected mode of the column. The results of this study are discussed in the following sections.

5. Column analysis

As an illustrative example a reinforced concrete column section 500 mm×500 mm with grade

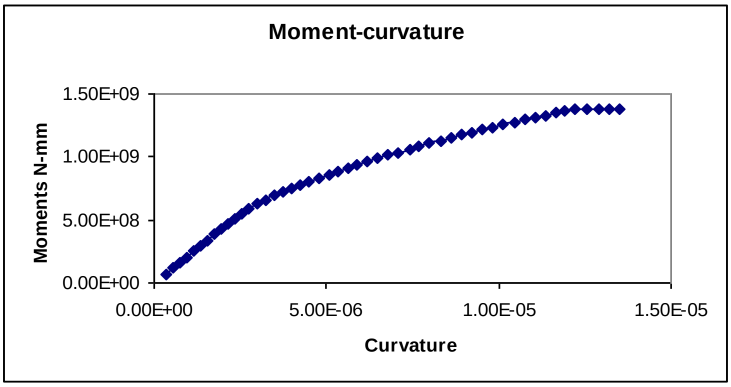

Fig. 7 Calculated moment-curvatures for the column section at $0.3P_o$

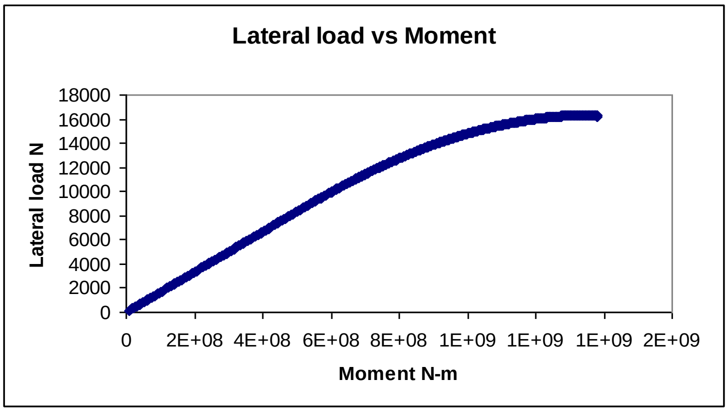

Fig. 8 lateral loads vs Moments at $0.3P_o$

of concrete, 80 MPa, contained 2.5 percentage of longitudinal reinforcement and slenderness ratio of 80, was selected. The entire length of the column was discretised into 20 equal segments and all nodes were subjected to the lateral wave loads varied hyperbolically from top to bottom nodes. The lateral wave loads were applied and incremented in terms of calculated wave load coefficients shown in Table 1. The lateral and vertical loads considered in this study are shown in Fig. 6. The lateral loads assumed in terms of wave load coefficients were incremented up to failure of the column under the vertical load of $0.3P_o$ where P_o is the squash load of the column section considered. The established moment- curvature relationships, the plotted graphs of lateral wave load H vs. moment, lateral wave load H vs. deflection and deflected shape of the column at failure are shown in Figs. 7-10 respectively. The maximum flexural strength of the column is 1380 kN-m and lateral wave resistance H at failure is 16.2 kN with the maximum deflection of 131.53 mm at failure load.

6. Summary of predicted results

For each column sections considered in this study, forty eight columns of different

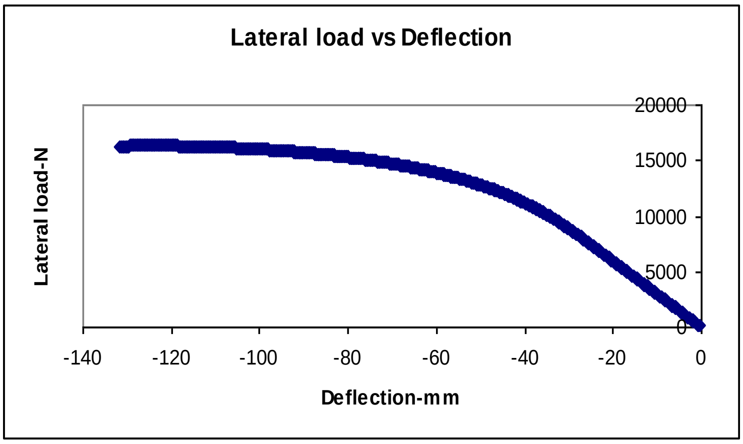

Fig. 9 Lateral loads vs deflection at $0.3P_o$

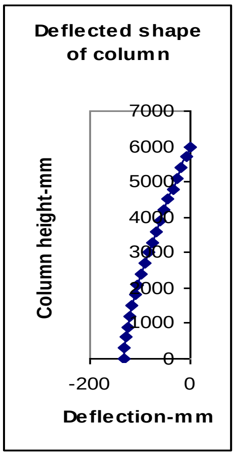

Fig. 10 Column mode at failure at $0.3P_o$

Table 3 Column 500×500 mm, Le/r=40, p=2.5%, f_c'=80 MPa

Vertical load Ratio (N/P_o)	Failure Lateral Load (kN)	Max Moment (kN-m)	Max Deflection (mm)
0.1	44.16	991.00	35.69
0.2	52.57	1220.00	31.68
0.3	58.57	1380.00	28.32
0.4	58.78	1410.00	24.90
0.5	56.73	1380.00	21.69
0.6	52.97	1320.00	19.45

Table 4 Column 500×500 mm, Le/r=60, p=2.5%, f_c'=80 MPa

Vertical load Ratio(N/P_o)	Failure Lateral Load (kN)	Max Moment (kN-m)	Max Deflection (mm)
0.1	26.80	991.00	82.55
0.2	30.23	1220.00	74.20
0.3	32.46	1380.00	67.32
0.4	31.41	1410.00	59.32
0.5	29.25	1380.00	51.82
0.6	26.03	1320.00	46.86

combinations of concrete compressive strengths, longitudinal reinforcement ratios and slenderness ratios were analyzed by the developed numerical procedure at various vertical loads ranging from 0.1 to 0.6 P_0 and the column sections were assumed to have the adequate lateral reinforcement of 12 mm diameter bars to confirm failure only in flexure. From the summaries of the results shown elsewhere, predicted results for the columns 500×500 mm having concrete compressive strength f_c'=80 MPa and longitudinal reinforcement ratio p=2.5% at slenderness ratios of 40, 60, 80 and 100 are given in Tables 3 to 6. The various comparative graphs of vertical load ratio versus lateral loads, moments and deflections for different concrete strengths, longitudinal reinforcement ratios and slenderness were drawn and shown in Figs. 11- 13.

Table 5 Column 500×500 mm, *Le / r*=80, *p*=2.5%, f_c'=80 MPa

Vertical load Ratio (N/P_o)	Max Lateral Load (kN)	Failure Lateral Load (kN)	Max Moment (kN-m)	Max Deflection (mm)
0.1	17.08	17.07	991.00	154.30
0.2	17.46	16.96	1220.00	141.82
0.3	16.35	16.22	1380.00	131.53
0.4	14.23	13.73	1410.00	117.53
0.5	11.75	11.04	1380.00	103.46
0.6	8.06	7.43	1320.00	94.63

Table 6 Column 500×500 mm, *Le / r*=100, *p*=2.50%, f_c'=80 MPa

Vertical load Ratio(N/P_o)	Max Lateral Load (kN)	Failure Lateral Load (kN)	Max Moment (kN-m)	Max Deflection (mm)
0.1	10.89	10.11	991.00	259.42
0.2	8.54	6.07	1220.00	252.94
0.3	6.86	1.27	1380.00	247.07
0.4	4.39	0.10	1410.00	198.10
0.5	0.79	0.09	1380.00	143.43
0.6	-	-	-	-

6.1 Effect of applied eccentric compression

It can be seen from a general observation from the summary of data, the lateral wave load resistance of the column increases with increasing the vertical loads up to certain level and then decreased for further increasing. It also indicates that flexural strength of the column section is increased with increasing the vertical load approximately up to 0.3P_0 to 0.4 P_0 depending upon the structural properties of the section and then the flexural strength of the section is decreased for further increase in vertical load on the column. The flexural strength of the columns are increased with increasing vertical thrust up to certain level due to the resulting direct compressive stress in concrete which will counter acts with the expected bending tensile stress induced by the external moments. The further increase in vertical thrust reduces the flexural strength of the columns due to increase in direct compressive stress in concrete which will reduce the availability of compressive resistance against the bending compression expected from the external moments. The flexural strength of the column section is normally depending on the structural properties of the section and vertical compression on the column. Assessing the flexural strength of the column section by moment-thrust-curvature approach is independent of the slenderness of the columns. The limit of compressive strain of the extreme concrete fibre from the neutral axis is controlled by the equilibrium condition of forces, ie the total internal forces due to concrete and reinforcing steel should be the same as applied vertical thrust. Obviously total internal moments of the section will be depending on the limitation of the extreme concrete fibre strains, which satisfies the equilibrium condition. Whereas the lateral loads resistance of the column depends on the flexural strength of the column section and also depends on slenderness of the column. Maximum lateral load resistance achieved at the vertical thrust of 0.2 P_0 to 0.3 P_0.

As an example, It can be clearly noted from calculated failure moments given in Tables 3-6, for column section 500 mm×500 mm having concrete compressive strength of 80 MPa and 2.5 percentage steel, the failure moments at the vertical load of 0.1 P_0 to 0.6P_0 are 991.0, 1220.0, 1380.0, 1410.0, 1380.0 and 1320.0 kN-m respectively for all the considered slenderness ratio of 40, 60, 80 and 100 but column of slenderness ratio 100 unable to support any further loads after 0.5 P_0. Whereas lateral load resistance for the same columns at the corresponding vertical loads are varying very considerably with slenderness ratio, mainly due to the combined effect of P-Δ parameters. The summary of the results of parametric study on all the cases indicates higher lateral load resistances are achieved at lower vertical thrust level than the vertical thrust level produce the maximum flexural strength for slender columns. It can be observed from the summary of the analyzed results all the column section considered in the parametric studies that the failure deflections are reduced while increasing the vertical thrust on the columns. It indicates that the ductility of the section is considerably reduced with increasing the vertical compression on the columns. Figs. 11 and 12 shows the failure moments and lateral strength at various vertical load ratios for the columns of slenderness ratio 80, percentage of steel 2.5% and concrete strength 40, 60, 80 and 100 MPa.

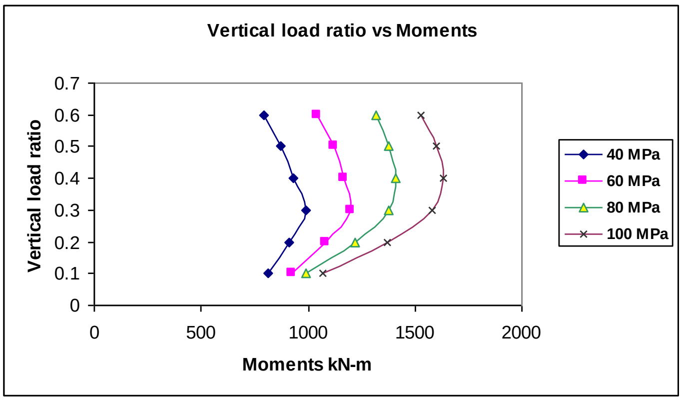

Fig. 11 *N/Po* vs Failure moment-Column 500×500, *Le/r*=80, *p*=2.5%

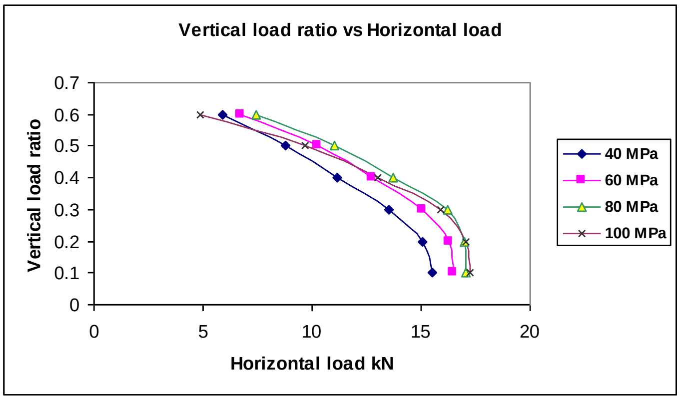

Fig. 12 *N/Po* vs Failure lateral load-Column 500×500, *Le/r*=80, *p*=2.5%

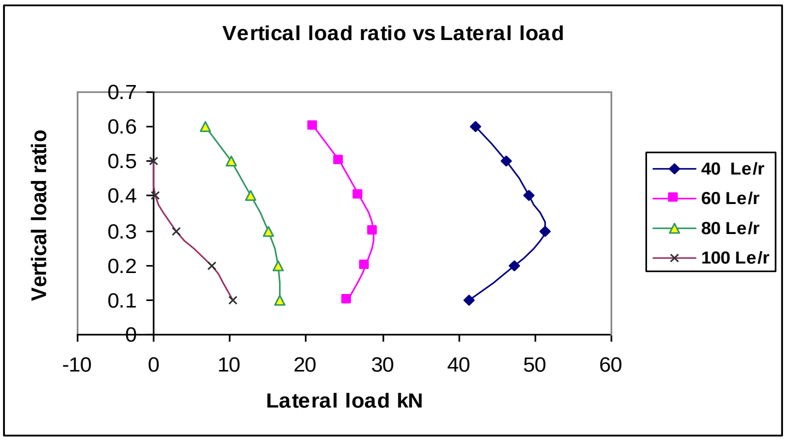

Fig. 13 *N/Po* vs lateral load-Column 500×500, f_c'=80MPa, p=2.5%

6.2 Effect of slenderness

The lateral load resistances of the column are directly affected by the slenderness of the columns by two ways. The increases in column lengths are resulting in increasing the lever the distances of lateral loads from the critical section at the bottom. Therefore the lateral force of the same magnitude will develop the greater moments for the more slender columns than short columns. Secondly the lateral load resistances are affected by increasing the secondary moments due to increase in deflections for more slender columns than short columns. It can be clearly noted from the summary of the results of all the cases considered in this parametric study that maximum lateral load resistances and failure lateral loads are the same for the columns of slenderness ratio of 40 and 60. The failure lateral loads are reduced little extend for the columns of slenderness ratio of 80. But the failure lateral loads are very sharply reduced to greater extend from the maximum lateral load resistances for the columns of slenderness ratio 100. From the Tables 5 and 6, it is clear that the failure lateral load is reduced by only 15.35% for column of slenderness 80 at the vertical load of 0.4P_0 whereas the failure lateral load is reduced by 92.13% for the column of slenderness 100 for the same condition due the increased effect of P-Δ parameters.

The comparative graphs of lateral load resistance of the columns with different slenderness ratios are plotted and shown in Fig. 13. From the results, it is clearly noted that for all the cases considered in the parametric studies, maximum lateral load resistance is achieved at vertical thrust in the range of 0.3 P_0 for the column of slenderness ratio 40 and 60. Whereas the vertical thrust in range of 0.2 P_0 is giving the maximum lateral load resistance for column of slenderness ratio 80. For columns of slenderness ratio 100, lateral load resistance is reduced even at very low range of vertical loads in order of 0.1 P_0. The trends of lateral load resistance with respect to vertical thrust are same for the columns of slenderness ratio 40 to 60 and have some acceptable changes in the trend up to slenderness ratio 80. But for the slenderness ratio 100, the reductions in lateral load resistance for increasing the vertical thrust are highly non-linear. The very slender columns of high strength concrete with less percentage of steel will fail at very low vertical thrust without capable of resisting any lateral loads.

7. Conclusions

The simplified wave impact load model enables practical applicability without involving tedious computational efforts and saves computational time and space. The wave load resistance and structural response of the columns subjected to eccentric compression could be assessed well by the developed computer based iterative numerical procedure. The failure deflections are reduced at higher vertical loads for all the columns of any slenderness ratios, compressive strengths and percentage of longitudinal reinforcements. The maximum flexural strength of the column sections are achieved at the vertical loads in the range of 0.3 P_0 to 0.4 P_0 depending on the combination of concrete strength and percentage of steel for all slenderness ratios. But the columns of high slenderness ratio in order 100 will have stability failure at very low vertical loads. The maximum lateral strength of the column sections are achieved at the vertical loads in the range of 0.2 P_0 to 0.3 P_0 depending on the combination of concrete strength and percentage of steel for the slenderness ratios less than 80. The columns having slenderness ratio more than 80 and subjected to higher vertical thrust will be under high risk of failure due to lateral loads of even a smaller magnitude in deflected mode.

References

ACI 318 (2008), Building Code Requirements for Reinforced Concrete (ACI 318-08), American Concrete Institute, Detroit.

Attard, M.M. and Stewart, M.G. (1997), “An Improved Stress Block Model for High Strength Concrete”, Research Report No. 154.10.1997, ISBN 0 725910070, The University of Newcastle, Australia.

Azizinamini, A., Kuska, S.S.B., Brungardt, P. and Hatfield, E. (1994), “Seismic behavior of square high strength concrete columns”, ACI Struct. J., **91**(3), 336-345.

Baudic , S.F., Williams, A.N. and Kareem, A. (2000), “A two-dimensional numerical wave flume: part 2-hydrodynamic loads and structural responses”, *Proceeding of ETCE/OMAE 2000 Joint conference Energy for the New Millennium*, New Orleans, February.

Berrera, A.C., Bonet, J.L., Romero, M.L. and Miguel, P.F. (2011), “Experimental tests of slender reinforced concrete columns under combined axial load and lateral force”, *Eng. Struct.*, **33**, 3676-3689.

Bouchaboub, M. and Samai, M.l. (2013), “Nonlinear analysis of slender high-strength R/C columns under biaxial bending and axial compression”, *Eng. Struct.*, **40**, 37-42.

Cambell, I.M.C. and Weynberg, P.M. (1979), “Slam load histories on cylinder”, Report No.416, Wolfson Marine Craft Unit, University of Southampton.

Collins, M.P., Mitchell, D. and MacGregor, J.G. (1983), “Structural design considerations for high- strength concrete”, *Concrete Int.*, **15**(5), 27-34.

Davies, K.B., Leverette, S.J. and Spillane, M.W. (1994), “Ringing of TLP and GBS platforms”, *Proceedings BOSS’94*, Cambridge, MA, 569-585.

Doran, B. (2009), “Numerical simulation os conventional RC columns under concentric loading”, *Mater. Des.*, **30**, 2158-2166.

Hugo, R., Humberto, V., Antonio, A. and Anibal,. C. (2012), “Comparative efficiency analysis of different nonlinear modeling strategies to simulate the biaxial response of RC columns”, *Earthq. Eng. Eng. Vib.*, **11**(4), 553-566.

Jayakumar. M., Thiagarajan, K.P. and Rangan, B.V. (2004)m “Response of high strength concrete columns / piles under wave impact loads”, *The International Conference on Structural and Foundation Failures*, Singapore, August.

Jayakumar. M. (2010), “Non-linear wave load model to predict the high frequency deep wave impact forces on offshore structures”, *International Conference on Advances in Interaction and Multiscale Mechanics,* *AIMM10*, Jeju, May-June.

Leite, L., Bonet, J.L., Miguel, P.F. and Fernondaz-Prada, M.A. (2013), “Experimental research on high strength concrete slender columns subjected to compression and uniaxial bending with unequal eccentricities at the ends”, *Eng. Struct.*, **48**, 220-232.

Morison, J.R., O’Brien, M.P., Johnson, J.W. and Schaff, S.A. (1950), “The force exerted by surface waves on piles”, *Petrol. Tran.*, *AIME*, **189**, 149-159.

Popovics, S. (1973), “A numerical approach to the complete stress-strain curve of concrete”, *Cement Concrete Res.*, **3**(5), 583-599.

Sarker, P.K., Adolphus, S., Patterson, S. and Rangan, B.V. (2000), “High strength concrete columns subjected to single or double curvature bending”, *PCI/FHWA/FIB Inetrnational Symposium on High Performance Concrete*, Orlando, September.

Sarpkaya, T. and Isaacson, M. (1981), “Mechanics of wave forces on offshore structures,” Van Nostrand Reinhold**.**

Zou, J. and Kim, C.H. (1995), “Extreme wave kinematics and impact loads on fixed truncated circular cylinder”, *Proceedings of Fifth International Offshore and Polar Engineering Conference*, The Hague, The Netherlands, June.